DOI: 10.1002/smll.200((……))

Mie and Bragg plasmons in sub-wavelength silver semi-shells**

Abbas I. Maaroof, Michael B. Cortie, Nadine Harris, and L. Wieczorek*

Two-dimensional arrays of silver semi-shells of 100 and 200 nm diameter display complex reflection and transmission spectra in the visible and near-infrared. Here we deconstruct these spectral features and demonstrate how they result from the coupling of incident light into a delocalized Bragg plasmon, and the latter's induction, in turn, of localized Mie plasmons in the arrays. These phenomena permit the excitation of transverse dipolar plasmon resonances in the semi-shells despite an ostensibly unfavorable orientation with respect to normally incident light. The resulting spectral feature in the mid-visible is strong and tunable.

Keywords:
- silver
- Bragg plasmon
- Mie plasmon
- nanophotonics
- optical properties

1. Introduction

The discovery of the anomalous transmission of light through opaque metal films containing a regular array of nanoholes[1,2] or through, or within, coatings comprised of a regular array of plasmonically active shapes such as nanowires,[3] semi-shells[4-11] or voids[12,13] has sparked widespread interest. This is because such structures may have potential applications in fields as diverse as nanophotonics,[14] sensing,[15] surface enhanced Raman scattering,[16] and optical filters.[17,18] The accepted explanation considered for such anomalous behavior is that the incident light couples via diffraction (scattering) into surface plasmon polaritons (SPPs) which then propagate across or along the coating through the holes or metallic nanostructures.[19,20] (Light does not normally couple to a *smooth* metal-air interface to produce a SPP because the SPP would have a momentum greater than the light at the same frequency.) The diffractive coupling with the new systems is made possible by prisms, gratings, or periodic sub-wavelength corrugations, bumps and holes.[2] The term 'Bragg plasmon'[12] has been used to describe SPPs like this, which interact with the periodic mesoscale structure as they travel through it. The Bragg plasmons are bound to the surface, and propagate only a short distance until their energy is dissipated, but this is sufficient to transport the light from one side of the coating to the other, or generate some useful lateral enhancement of the electric field. As a result of the foregoing, it is now well known that these systems display anomalous transmission and reflection spectra compared to those of a flat metal surface with the same coverage of metal.[4,6-8,10-13]

Coatings comprised of Au or Ag on a colloidal crystal template are particularly convenient systems with which to explore the coupling of light into and out of SPPs. This is both because they have a plasmon resonance in the visible portion of the spectrum and because they are noble (i.e. they are resistant to oxidation).These systems, albeit usually with somewhat larger spheres, are also excellent substrates for

[*] Dr. A.I. Maaroof ,Prof. M.B. Cortie, Mrs N. Harris
Institute for Nanoscale Technology
University of Technology Sydney
PO Box 123, Broadway NSW 2007 (Australia)
Fax: (+61)2-9514-8349
E-mail: michael.cortie@uts.edu.au

Mr. Lech Wieczorek
Commonwealth Scientific and Industrial Reseach Organisation
Lindfield NSW 2070 (Australia)

Supporting information for this article is available on the WWW under http://www.small-journal.org or from the author

Surface Enhanced Raman spectroscopy, a capability that has been well-explored by the Van Duyne group.[16,21] They may also have value as the basis of a refractometric sensor.[4,22] Ordered 2D arrays of semi-shells based on Au[6,8,11-13] and Ag[7,10] have also been investigated purely on account of their interesting optical properties. Most of the past work cited above, however, has been directed at semi-shells with internal diameters similar to the wavelengths of visible light and/or has been focused on SERS. Our interest, by contrast, is in the analysis of plasmonic phenomena in structures with *sub-wavelength* periodicities. In either case, the semi-shells in these arrays may also be subsequently separated from one another and will then exhibit quite different optical properties compared to when in contiguous form, [6,23,24] a point which we also address here.

Arrays of silver semi-shells were prepared by depositing silver at an oblique angle and at various thicknesses onto a rotating substrate covered with a close-packed monolayer of 100 or 200 nm diameter polystyrene nanoparticles (PSNs). This is based on the 'nanosphere lithography' technique[25] with the important difference that it is the deposit on top of the template that is of interest in the present work, rather than any little pillars or crescents of metal developed underneath it on the substrate. Further details are given in the experimental section.

2. Results and Discussion

2.1. Characterization of arrays

Figure 1 shows a scanning electron microscope (SEM) image of a resulting array of silver semi-shells. The ordered domains are some 10 to 50 μm in width (Supporting Information, Figure S1).

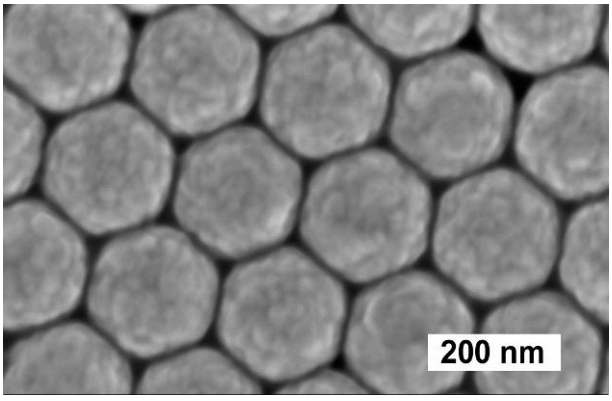

Figure 1. SEM image of silver semi-shells of nominal 30 nm section thickness deposited onto a 2D hexagonal closed-packed array of polystyrene nanoparticles of nominal 200 nm diameter. The substrate is super white glass.

Figures 2(a) and (b) show a typical transmittance spectrum collected at normal incidence ($\theta = 0°$) and a reflectance spectrum (measured at near normal incidence of 8°) respectively, for a coating of 20 nm Ag on a monolayer of 200 nm diameter PSNs. The inset graph shows the absorptance, given by $A = 1 - T - R$. Also shown is the baseline: a 20 nm silver film on the glass substrate alone. A 20 nm thick coating of Ag was chosen as the basic comparator in the present work because this is roughly the depth to which light penetrates silver in the visible part of the spectrum.[17,26] Observance of this criterion is considered desirable in order to maximize the generation of surface plasmon-polaritons.[26] The differences between the spectra for the smooth silver film and that of the semi-shell array can be attributed, in an empirical way, to the appearance of the following phenomena in the array: (1) suppressed reflectivity around 370 and 550 nm but increased reflectivity at around 420 nm, and (2) increased absorption at around 350 and 525 nm. The net effect on the transmitted light (compared to the smooth silver film) is to cause anomalously low transmission through the array structure at around 340 nm and 470 nm. However, the transmittance far from those wavelengths is qualitatively similar to that of the flat Ag film. Therefore, in order to explain the difference between the optical properties of this array and an ordinary silver film, it is necessary to establish the occurrence of one or more phenomena that occur in the array coating at wavelengths between 340 to 370 nm, and between 470 to 530 nm, but which are absent in the ordinary Ag film.

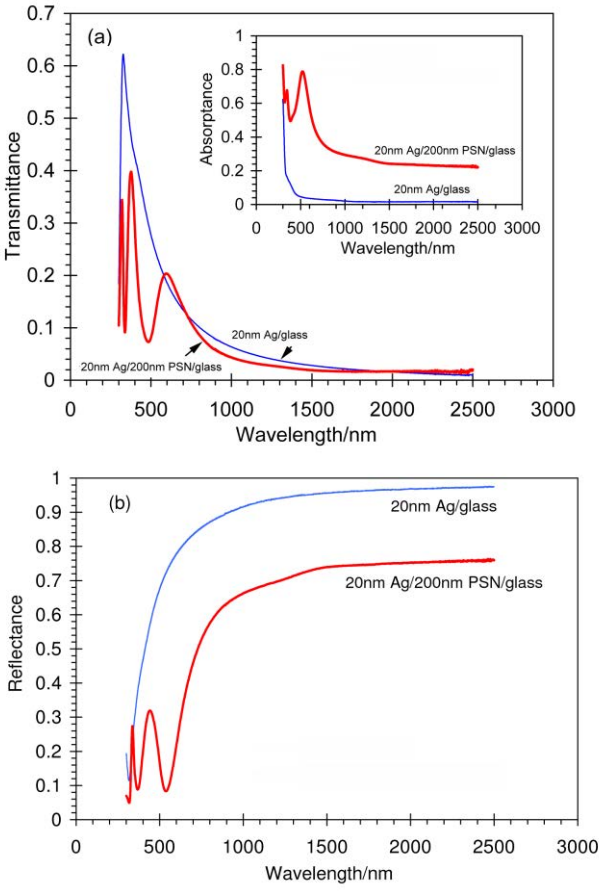

Figure 2. Shows typical (a) transmittance and (b) reflectance for 20 nm thick semi-shells on ~200 nm polystyrene spheres on a glass substrate. The properties of an equivalent flat silver film on glass are shown for comparison. The transmittance shows a narrow distinct feature peak at λ=320nm typical for bulk films. Inset graph shows deduced absorptance.

The corresponding data for the coating produced by depositing various thicknesses of Ag onto a monolayer of 100 nm diameter PSNs are shown in the Supporting Information (Figure S2). The results are qualitatively similar to those for the 200 nm diameter PSNs, but the change in diameter (and associated decrease in aspect ratio) caused the prominent 490 nm absorption peak of the 200 nm array to be shifted to about ~420 nm in the 100 nm array. On the other hand the absorptance peak at ~350 nm was not materially effected.

Some insight into the operative phenomena can be gained by considering the optical properties of other arrays prepared from the polystyrene spheres, but in which systematic substitutions in materials were made. For example, the polystyrene monolayers alone showed only a monotonically decreasing and negligible absorption in the visible, with only a faint indication of slightly increased reflectivity between 420 and 600 nm, relative to other wavelengths (Supporting Information, Figure S3). This result is in contrast to that of Farcau and Astilean[7] who found that, in their experiment, the monolayers of bare polystyrene spheres interacted significantly with the incident light by what they described as 'resonant coupling into the first waveguide mode' of the monolayer. The criterion for this interaction is given by the parameter z

$$z = \sqrt{3}.a/\lambda \ , \ z > 0.7 \qquad (1)$$

where a is the radius and λ the wavelength.[27] In the present samples (where $\varepsilon \approx 1.46$ and $a \approx 50$ or 100 nm) this is attained only when $\lambda < 225$ nm and therefore well out of the part of the spectrum investigated. Therefore, the phenomena observed in the present Ag-coated array at ~360 nm and ~530 nm are certainly not due to diffraction off the PSNs alone.

Next we consider whether simple periodic modulation of the dielectric properties of the coating layer might be responsible. It is well-known that the application of materials of high dielectric constant, such as Si[28] or Ni onto ordered PSN arrays produce structures with complex optical spectra, with transmission peaks due to diffractive effects given by[10]

$$\lambda_{SP} \approx \frac{\sqrt{3}d\sqrt{\frac{\varepsilon_m \varepsilon_d}{\varepsilon_m + \varepsilon_d}}}{2\sqrt{m_1^2 + m_2^2 + m_1 m_2}} \qquad (2)$$

where λ_{SP} is the peak wavelength of the anomaly, ε_m and ε_d are the dielectric properties of the coating and sphere respectively, and m_1 and m_2 are integers. However, once again, because the present PSN are smaller than those used by most prior investigators, first-order or second-order examples of such peaks generated by equation (2) would only be expected at $\lambda < 300$ nm. We also verified this experimentally : transmission through a Si-coated PSN array exhibited a smooth transition from low to high between ~500 and 700 nm. The reflectivity spectrum was relatively featureless, with a broad, low peak at about 440 nm (Supporting Information, Figure S4). Similarly, the optical properties of a SiO_2-coated array of PSNs displayed little of interest (Supporting Information, Figure S5). Therefore, the sharp features observed on the spectra of the Ag-coated array in Figure 2 (or Figure S2) are not likely to be due to a simple grating-like modulation of the coating's refractive index either. The lack of such features on the spectrum of the ordinary flat Ag film on glass also eliminates thin film stack effects as a possible explanation.

Instead, evidence in support of the contention that the features on the optical spectra are due to one or more plasmon resonances was obtained by over-coating the Ag semi-shell arrays with Al_2O_3 or SiO_2. This would be expected to red-shift a plasmon resonance, but have only a modest effect on any purely diffractive phenomena. The results are given in the Supporting Information (Figures S6 and S7) and show the expected red shift. Therefore it is certainly feasible, on this basis, to attribute the strong absorbance peaks at 400 and 490 nm in the 100 and 200 nm arrays respectively to a plasmon resonance.

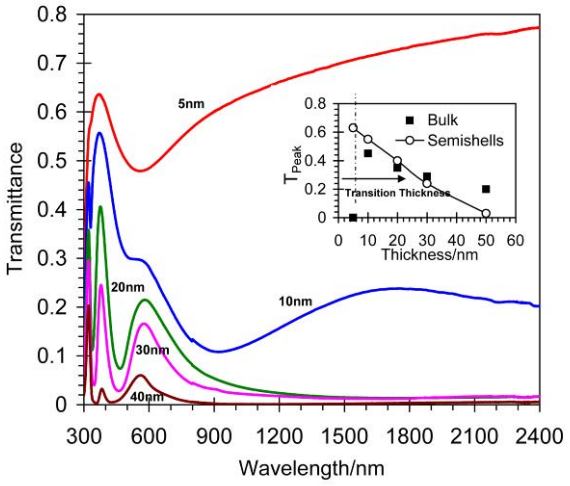

Figure 3. Transmission spectra for 2-D arrays of semi-shells of 200 nm inside diameter and with various thicknesses of Ag. The most remarkable aspects are that the samples which are coated with 20 nm or more of Ag show an anomalous peak in their transmission spectra at about 550 nm and low transmittance in the near-IR, whereas in contrast the sample coated at 5 nm is virtually transparent in the near-IR. Inset graph shows, however, that the transmittance at ~325 nm is simply proportional to the thickness and therefore not due to a plasmonic or diffractive phenomenon.

Varying the thickness of silver in the semi-shell arrays also had a pronounced effect on their optical properties (Figures 3 and 4, and Figure S2 in the Supporting Information). Some of this effect is due simply to attenuation; this is evident if the transmission at ~325 nm is considered in the 200 nm array (Figure 3, inset). At this wavelength the transmission through the array, and its variation with thickness, is very similar to that through a flat Ag film, and follows the same trend with thickness. The more interesting phenomena are rather the two anomalously high absorptances identified earlier for the 200 nm structure at ~350 nm and ~525 nm, now shown in Figure 4 for various coating thicknesses. The first absorptance peak is not visible on the spectrum for the 5 nm thick coating because in that case it is masked by the strong absorption due to the interband transitions of silver. However, it is slightly red-shifted by an increase in coating thickness, reaching 363 nm for the 50 nm thick coatings. The second peak is strongly blue-shifted as the coating thickness is increased, starting at 601 nm for the 5 nm thick coatings, and moving to only 544 nm for the high thickness coatings. The threshold thickness

for percolation in Ag films is about 10 nm,[29] and a transition in the optical response from one due to localized surface plasmon resonances on individual blebs of sputtered Ag, to one due to delocalized surface plasmon-polaritons is observed when percolation is achieved. This is particularly obvious in the near-infrared reflectivity, which changes from low to high as the percolation threshold is crossed (Figure 4a)

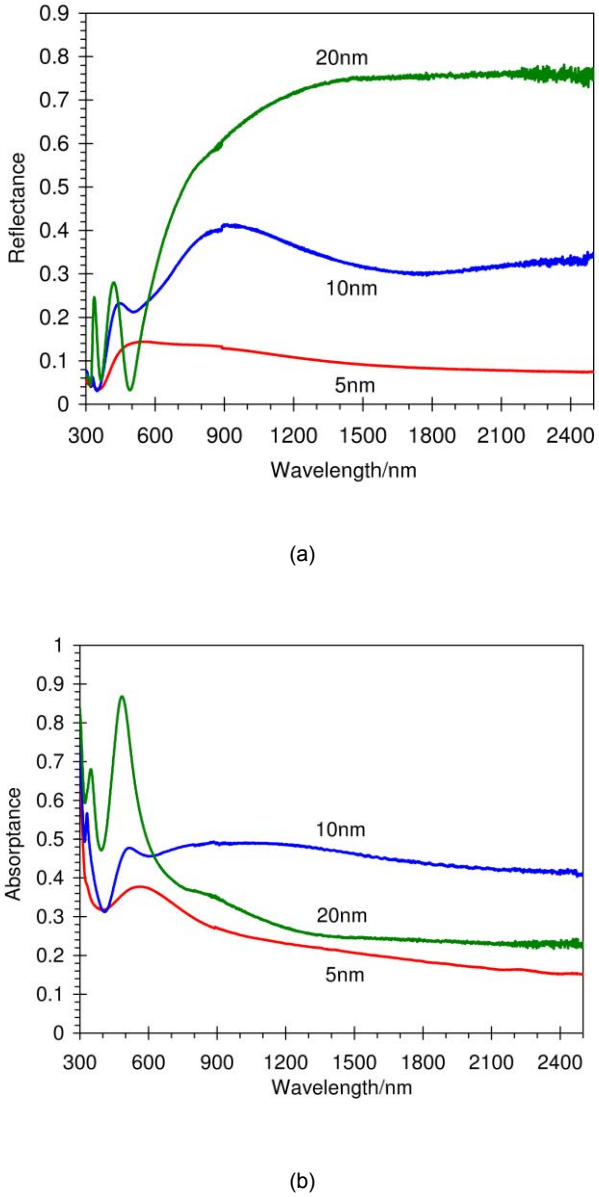

Figure 4. (a) Reflectance and (b) absorptance spectra of arrays of semi-shells with ~200 nm diameter cores and different thicknesses of Ag, showing rather different modes of plasmon resonance. There is a significant growth and strengthening of the absorption peak at about 500 nm as the coating of Ag becomes continuous and thicker.

Since Bragg plasmons are longitudinal modes confined to the surface,[30] the direction and extent to which they are excited will depend on the polarization of the incident light and its orientation with respect to the close-packed direction of the array.[31] The effect of polarization is clearly observed for the present samples, in which it is seen that an increase in the angle of incidence of p-polarised light causes a decrease in the width, and red-shift in the position, of the prominent *transmittance* peak originally at 380 nm (Figure 5a). This must be due to a corresponding increase in either or both *absorptance* or *reflectance* at about 350 nm. On the other hand, only attenuation of the transmission peak occurs when the same experiment is carried out with s-polarized light (Figure 5b). Attenuation of the peak, without a shift in its wavelength, is simply the result of the light having to transverse a greater thickness of coating when at higher angles of incidence. However, no effect of azimuthal rotation of the substrate is observed (Supporting Information, Figure S8) because the beam size of the spectrophotometer is so large as to effectively average out the effect of the varied orientations of the individual domains.

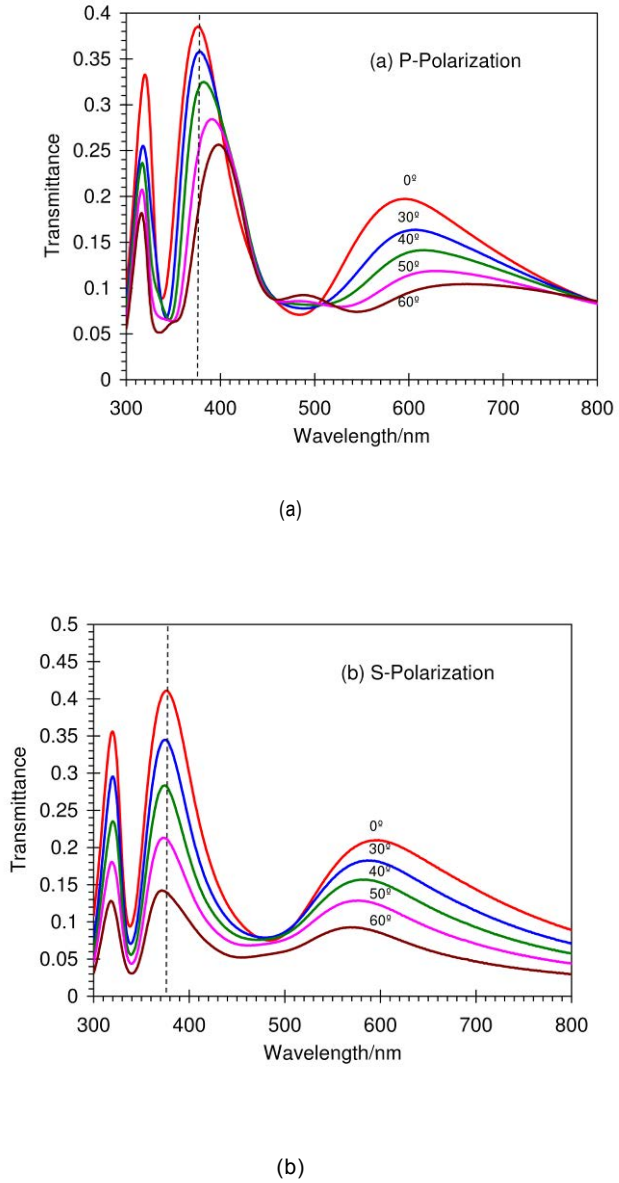

Figure 5. Transmittance spectra of the sample in Figure 2 measured at different angles of incidence. (a) p-polarized light (b) s-polarized light.

2.2. Numerical simulation of optical properties

Some further insight into the situation may be gained by numerical simulations of the optical properties. Here we have used a code based on the discrete dipole approximation[32,33] and for which input targets are generated as described elsewhere.[34] Of course the real semi-shells are complex shapes and some simplifying assumptions must be made in order to do the calculations. Furthermore, it is not currently feasible to simulate a whole array of such comparatively large nanostructures; however, individual semi-shells can certainly be simulated.

In Figure 6 we show the simulated extinction and absorption efficiencies of a smooth Ag hemisphere of 140 nm ID and 180 nm OD, on a polystyrene core. This shape was chosen because it is intermediate in nature between the 100 and 200 nm semi-shells produced experimentally. The results for the two important orientations of the electric field are shown, and each orientation generates a rather different plasmon mode; these have been defined elsewhere as the α and β modes.[35] The α is a simple dipole, i.e. transverse, oscillation, while the β mode may be considered to be a longitudinal oscillation. An animation of the α resonance in semi-shells of 100 nm inside diameter is provided in the Supporting Information as an AVI file. The effect of surface roughness, and the effect of multiple particle orientations are examined in Figure 7. Adding roughness to the outer surface of the hemisphere causes some broadening of the peaks and a red-shift of some 20 nm, but it not otherwise significant. However, comparison of the peaks in Figures 6 and 7 show that the inclusion of the polystyrene core in the calculations of Figure 6 caused a significant red-shifting of all of the main resonance modes. There is also a third mode evident, at about 400 nm, which we do not discuss further here (but see Cortie and Ford[35]). The various kinds of targets are shown as insets.

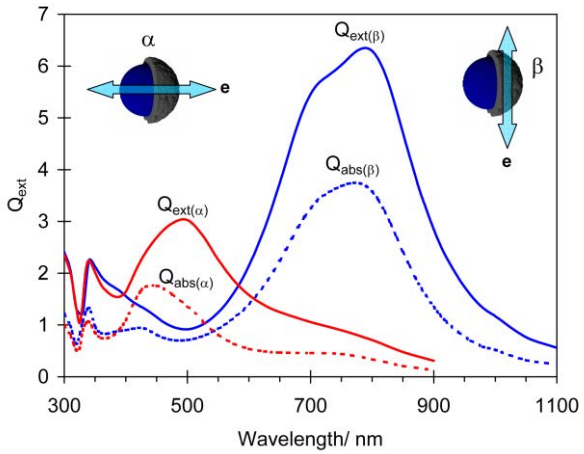

Figure 6. Effect of polarization on the absorption and extinction efficiencies of a 140 nm inside diameter, 180 nm outside diameter Ag semi-shell, calculated taking into account the presence of a spherical polystyrene core.

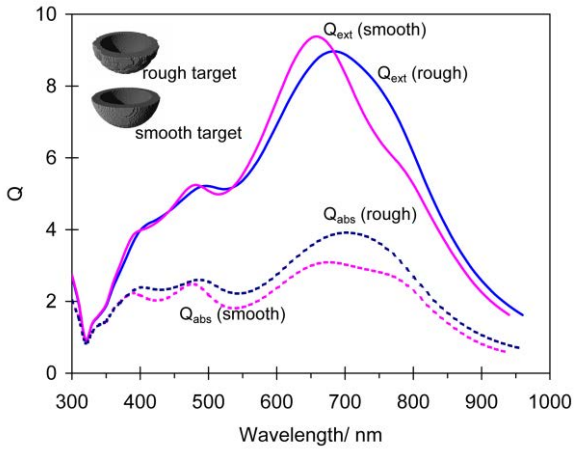

Figure 7. Effect of surface roughness on absorption and extinction efficiencies of a 140 nm ID, 180 nm OD Ag semi-shell, averaged over 125 target orientations.

It is evident that the action of the p-polarized light on the array (Figure 5a) can be qualitatively explained by an increased strength of the α resonance as the angle of incidence increases. However, this mode would not be expected in the first instance to be active in the *array* when the light is normally incident[35] because the polarization of the light would be at 90° to the direction of α dipole oscillation, and could therefore not excite it. However, coupling would be expected as the angle of incidence of p- (but not s-) polarized light was increased. On the other hand, the strong β (longitudinal) plasmon mode expected for a semi-shell presented at right angles to light[35] might have been expected, but is clearly absent in these coatings. These observations are consistent with a explanation in which the incident beam (and its polarization) is diffractively coupled into the array and partially rotated into the form of laterally propagating Bragg plasmons.[2,9,19,26,30]

Therefore, to verify that the β resonance is actually suppressed in the array, and to confirm its nature, we both measured and simulated the extinction spectra when the nominally 200 nm, 20 nm thick Ag semi-shells were liberated from the substrate and taken up into suspension in CH_2Cl_2 (Figure 8). When in suspension the semi-shells will certainly respond as discrete particles. [11,24,35,36] There is a resonance mode at ~530 nm and a very strong one at ~1100 nm in the present semi-shells, and excellent agreement between the measured and calculated spectra. Calculations were carried out with three model geometries (See figure caption). Irrespective of the geometric model used, it is clear that the discrete semi-shells display a major resonance at about 1000 to 1100 nm that is absent in the contiguous array from which they were liberated. The best matching model was the one with the irregular rim, the effect of which was to broaden, attenuate and red shift the plasmon resonances.

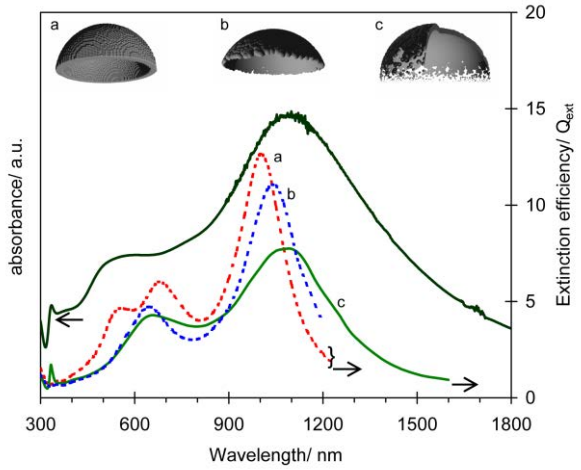

Figure 8. Comparison of measured absorbance and calculated optical extinction coefficients for three types of hollow Ag semi-shells of 200 nm inner diameter, suspended in CH_2Cl_2 .Three models were used in the simulations, a. simple hemisphere, b. tapered wall thickness with loose material around rim removed, c. tapered target, loose material around rim left in place, target cut away to show internal structure.

These results strongly suggest that the prominent absorption peaks at 400 and 490 nm for the arrays deposited on the 100 and 200 nm cores respectively are due to alpha resonances. Simulations of the α resonance in various models of semi-shells are shown in Figure 9 along with the corresponding experimentally determined absorptivity. It is clear that the basic form of the experimental data for the 100 nm core semi-shells can be well simulated with appropriate polystyrene-cored semi-shell models. The match for the semi-shells of ~200 nm diameter is not as good. This may be due to the effect of plasmons in neighboring semi-shells, acting in concert to reinforce the alpha resonance, and suppressing any multipole resonances that would otherwise broaden the absorptance peak.

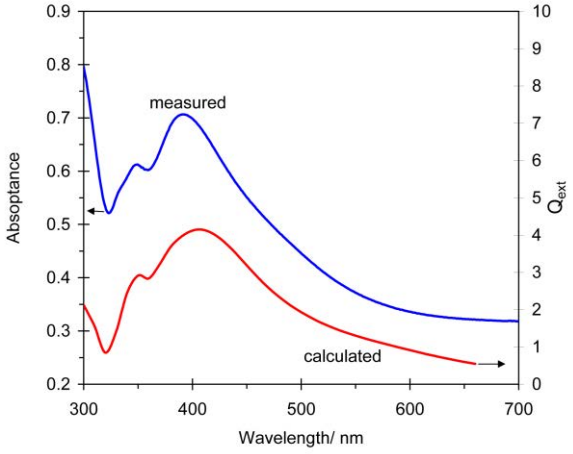

(a)

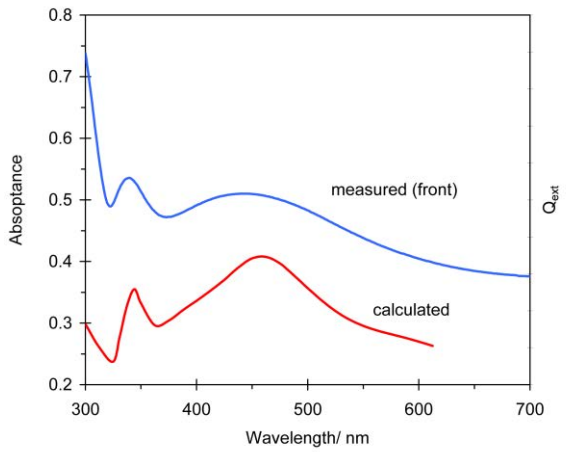

(b)

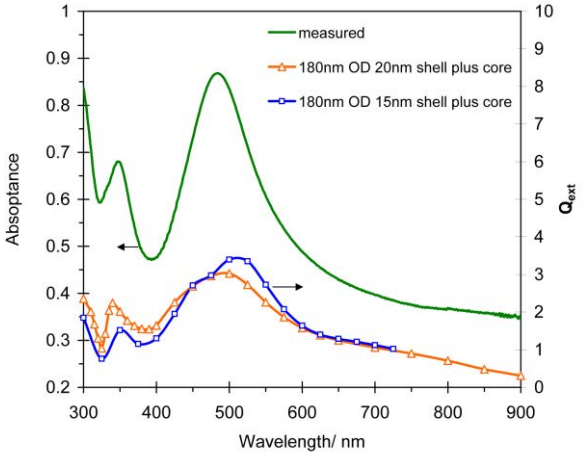

(c)

Figure 9. Close correlation between calculated and measured α plasmon resonances in Ag semi-shells of the present work. (a) data for 30 nm Ag semi-shells formed on 100 nm diameter polystyrene cores, calculation is for a 100 nm polystyrene hemispherical core, coated with a 30 nm shell of Ag (b) measured data for a sample with thinner wall thickness (*cf.* Figure S2 in Supporting Information) with a calculation based on a tapered shell profile (c) data for 200 nm polystyrene cores with simulations based on hemispherical semi-shells..

Finally, the disappearance of the β resonance in the array can be explained by the fact that it is a localised (*i.e.* Mie) resonance. When adjacent shells are connected by a sufficiently thick neck of silver the charge oscillation simply propagates across the neck, from shell to shell, *i.e* it becomes a Bragg plasmon with a very much red-shifted resonance condition. This is readily seen in simulations of the optical properties of structures comprised of one, two and three contiguous semi-shells, Figure 10. The structure is simulated in vacuum and has a 100 nm inner diameter and a 20 nm tapered shell. The β resonance of a single shell is at

about 600 nm in this case, but is increasingly shifted out to the near-infrared in the two- and three-shell arrays. It is feasible in our opinion to consider that it will be further shifted to well beyond 3000 nm in an array of several semi-shells. Regrettably, however simulations of such big systems lie beyond the capability of the hardware and software that we are currently using. Note, however, that propagation of the β resonance from semi-shell to semi-shell requires a contiguous metallic connection between them (Supporting Information, Figure S9).

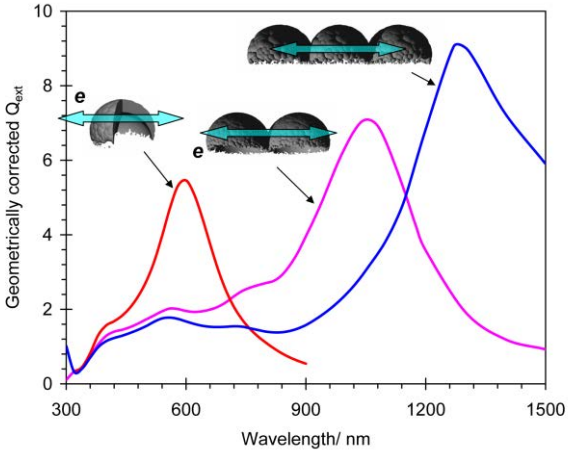

Figure 10. Simulation of the optical properties of one-, two- and three-shell arrays for normally incident light (and a longitudinally oriented electric field). The β resonance of the single shell is red-shifted into the near-infrared by the addition of adjacent shells.

3. Conclusions

Well ordered, two-dimensional arrays of nanoscale silver semi-shells may be readily fabricated by nanosphere lithography. The arrays have rich optical characteristics due to the excitation of different types of plasmon modes. The dominant far-field effect is due to a dipolar plasmon resonance in individual semi-shells but excitation of this mode can only be explained if the incident light was coupled to, and rotated 90º by, a Bragg plasmon in the plane of the array. The optical effects can be tuned by controlling the thickness of silver deposited, by selection of the nanosphere starting diameter, or by over-coating with other, non-plasmonic, dielectrics. Furthermore, the unique dispersion behavior also depends on the inclination and polarization of the incident light. The new insights into, and control of, these fascinating nanostructures may facilitate their exploitation in novel technological applications.

4. Experimental Section

Monodisperse spherical polystyrene particles of 100 and 200 nm diameter were obtained from Spherotech Inc. The nanospheres were diluted 1:2 (v/v) in a solution (1:400 v/v) of Triton X-100 in methanol. 10 μL of the diluted suspension was spin-cast at 2000 rpm onto optically polished super-white glass (20 x 20 x 1 mm^3) substrates from ProScientific. 'Super-white' glass are exceptionally flat and parallel, with a clean, wettable surface and possess optimum light transmission with minimum fluorescence or intrinsic colour. The glass had been previously ultrasonically cleaned with detergent solution for 20 minutes, rinsed with distilled water, and dried with high purity nitrogen gas. Single layer, thin films of Ag were deposited using high vacuum, DC magnetron sputtering. The sputtering target was a 99.999% Ag disc (50 mm diameter), placed 150 mm away from the substrate. The substrate was rotated 10 rpm and placed at 50° to the flux of silver. The base pressure was better than ~$1x10^{-4}$ Pa (~10^{-6} Torr), while sputtering was carried out in presence of flowing Ar, at a pressure of 0.3 Pa. Surfaces exposed at right angles to the flux of Ag received the full thickness of coating, but obviously this thinned towards the edges of the spheres, with thickness $t \propto \cos(\theta)$, where the θ designates the inclination of the particle surface with respect to the deposition direction. As a consequence, this effect leads to the individual silver caps being joined around their equators by only a bridge of Ag, as shown in Figure 1. The grain size in the Ag coating was of the order of 20 nm. Measurements of transmittance $T(\lambda)$ and reflectance $R(\lambda)$ were carried out using a Perkin-Elmer Lambda 950 UV/VIS/NIR spectro-photometer over the visible and near-infrared wavelength range 300 nm < λ < 2500 nm. Reflectance was measured at the near-normal incidence angle of θ=8°. The optical response of the samples was measured over the visible and near-infrared wavelength range, 300 nm < λ < 2500 nm. Both transmittance, T(λ), and reflectance, R(λ), were determined in order that the absorptance, A(λ), could be determined via

$$A(\lambda) = 1 - R(\lambda) - T(\lambda)$$

An anomalous increase in absorptance is an indicator of the probable presence of a plasmon.[29] The thickness of film deposited was determined with calibration of the system, with respect to the deposition angle of 50°.

The simulations of optical properties were performed with the DDSCAT program of Draine and Flatau.[32] This breaks up an arbitrary, nanoscale target into notional dipoles, and then solves for the extinction, absorption and scattering efficiencies numerically. The process is slow for larger targets and especially so when they contain materials (such as metals) with large dielectric constants. Convergence is abetted by having as small a dipole volume as is practicable. In this work dipole volumes of between 3 and 10 nm^3 were used, necessitating the generation of targets with between 50, 000 and 250,000 dipoles.

Acknowledgements

The authors thank Mr G. McCredie for technical assistance. Computational resources were provided under the merit allocation schemes of ac3 (in NSW) and the National Facility, APAC. This project was equally supported by Commonwealth Scientific and Industrial Research Organisation (Australia) and the University of Technology Sydney.

Received: ((will be filled in by the editorial staff))
Published online on ((will be filled in by the editorial staff))

[1] T. W. Ebbesen, H. J. Lezec, H. F. Ghaemi, T. Thio, P. A. Wolff, *Nature* **1998,** *391*, 667-669.

[2] W. L. Barnes, A. Dereux, T. W. Ebbesen, *Nature* **2003,** *424*, 824-830.

[3] A. Christ, T. Zentgraf, S. G. Tikhodeev, N. A. Gippius, J. Kuhl, H. Giessen, *Phys. Rev. B* **2006,** *74*, 155435.

[4] H. Takei, M. Himmelhaus, T. Okamoto, *Opt. Lett.* **2002,** *27*, 342-344.

[5] H. Takei, *J. Vac. Sci. Technol. B* **1999,** *17*, 1906-1911.

[6] C. Charnay, A. Lee, S. Man, C. E. Moran, C. Radloff, R. K. Bradley, N. J. Halas, *J. Phys. Chem. B* **2003,** *107*, 7327-7333.

[7] C. Farcau, S. Astilean, *J. Opt. A: Pure Appl. Opt.* **2007,** *9*, S345-S349

[8] P. Zhan, Z. Wang, H. Dong, J. Sun, J. Wu, H.-T. Wang, S. Zhu, N. Ming, J. Zi, *Adv. Mater.* **2006,** *18*, 1612–1616.

[9] F. Pigeon, I. F. Salakhutdinov, A. V. Tishchenko, *J. Appl. Phys.* **2001,** *90*, 852-859.

[10] L. Landström, D. Brodoceanu, K. Piglmayer, D. Bäuerle, *Applied Physics A. Materials Science & Processing* **2006,** *84*, 373–377.

[11] J. Liu, B. Cankurtaran, L. Wieczorek, M. J. Ford, M. B. Cortie, *Adv. Func. Mater.* **2006,** *16*, 1457-1461.

[12] T. A. Kelf, Y. Sugawara, R. M. Cole, J. J. Baumberg, M. E. Abdelsalam, S. Cintra, S. Mahajan, A. E. Russell, P. N. Bartlett, *Phys. Rev. B* **2006,** *74*, 245415.

[13] R. M. Cole, Y. Sugawara, J. J. Baumberg, S. Mahajan, M. Abdelsalam, P. N. Bartlett, *Phys. Rev. Lett.* **2006,** *97*, 137401.

[14] J. B. Pendry, *Science* **1999,** *285*, 1687-1688; H. J. Lezec, A. Degiron, E. Devaux, R. A. Linke, L. Martin-Moreno, F. J. Garcia-Vidal, T. W. Ebbesen, *Science* **2002,** *297*, 820.

[15] A. J. Haes, W. P. Hall, L. Chang, W. L. Klein, R. P. V. Duyne, *Nano Lett.* **2004,** *4*, 1029-1034; A. D. McFarland, R. P. Van Duyne, *Nano Lett.* **2003,** *3*, 1057-1062.

[16] J. A. Dieringer, A. D. McFarland, N. C. Shah, D. A. Stuart, A. V. Whitney, C. R. Yonzon, M. A. Young, X. Zhang, R. P. V. Duyne, *Faraday Discussions* **2006,** *132*, 9-26.

[17] J. R. DiMaio, J. Ballato, *Opt. Exp.* **2006,** *14*, 2380-2384.

[18] M. B. Cortie, X. Xu, M. J. Ford, *Phys. Chem. Chem. Phys.* **2006,** *8*, 3520-3527.

[19] W. L. Barnes, W. A. Murray, J. Dintinger, E. Devaux, T. W. Ebbesen, *Phys. Rev. Lett.* **2004,** *92*, 107401.

[20] J.-Y. Chu, T.-J. Wang, J.-T. Yeh, M.-W. Lin, Y.-C. Chang, J.-K. Wang, *Appl. Phys. A* **2007,** *89*, 387-390.

[21] C. R. Yonzon, D. A. Stuart, X. Zhang, A. D. McFarland, C. L. Haynes, R. P. Van Duyne, *Talanta* **2005,** *67*, 438-448.

[22] C. R. Yonzon, E. Jeoung, S. Zou, G. C. Schatz, M. Mrksich, R. P. V. Duyne, *J. Am. Chem. Soc.* **2004,** *126*, 12669-12676.

[23] J. Liu, B. Cankurtaran, G. McCredie, M. Ford, L. Wieczorek, M. Cortie, *Nanotechnology* **2005,** *16*, 3023-3028.

[24] J. Liu, A. I. Maaroof, L. Wieczorek, M. B. Cortie, *Adv. Mater.* **2005,** *17*, 1276-1281.

[25] J. C. Hulteen, R. P. Van Duyne, *J Vac Sci Technol A* **1995,** *13*, 1553-1558.

[26] W. L. Barnes, *J. Opt. A: Pure Appl. Opt.* **2006,** *8*, S87–S93.

[27] Y. Kurokawa, H. Miyazaki, Y. Jimba, *Phys. Rev. B* **2002,** *65*, 201102.

[28] L. Landström, N. Arnold, D. Brodocean, K. Piglmayer, D. Bäuerle, *Appl. Phys. A. Materials Science & Processing* **2006,** *83*, 271-275.

[29] A. I. Maaroof, G. B. Smith, *Thin Solid Films* **2005,** *485*, 198-206.

[30] F. J. García de Abajo, *Reviews of Modern Physics* **2007,** *79*, 1267-1290.

[31] E. Altewischer, M. P. van Exter, J. P. Woerdman, *Nature* **2002,** *418*, 304-306.

[32] B. T. Draine, in *Light Scattering by Nonspherical Particles: Theory, Measurements, and Geophysical Applications*, (Eds: M. I. Mishchenko, J. W. Hovenier, L. D. Travis), Academic Press, New York **2000**, 131-145.

[33] B. T. Draine, P. J. Flatau, *J. Opt. Soc. Am. A* **1994,** *11*, 1491-1499; B. T. Draine, P. J. Flatau, User Guide for the Discrete Dipole Approximation Code DDSCAT 6.1, http://arxiv.org/abs/astro-ph/0309069, January 2005.

[34] K. E. Peceros, X. Xu, S. R. Bulcock, M. B. Cortie, *J. Phys. Chem. B* **2005,** *109*, 21516-21520.

[35] M. B. Cortie, M. J. Ford, *Nanotechnology* **2007,** *18*, 235704.

[36] J. Liu, K. E. McBean, N. Harris, M. B. Cortie, *Mater. Sci. Engng. B* **2007,** *140*, 195-198.

Entry for the Table of Contents

full

Ordered arrays of nanoscale Ag semi-shells on polystyrene nanoparticle templates have rich and complex optical characteristics in the visible part of the spectrum, the origin of which has hitherto been somewhat uncertain. We demonstrate here that the most prominent absorption phenomenon is due to rotation of incident light into the plane of the array, with the subsequent excitation of an out-of-plane dipole plasmon resonance.

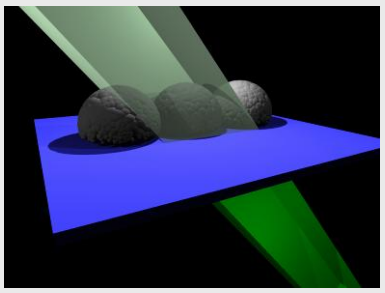

Plasmonics and nanophotonics

Abbas I. Maaroof, Michael B. Cortie*
Nadine Harris, Lech Wieczorek____**Page No. – Page No.**

Mie and Bragg plasmons in sub-wavelength silver semi-shells

Supporting Information

Mie and Bragg plasmons in sub-wavelength silver semi-shells

Abbas I. Maaroof, Michael B. Cortie, Nadine Harris, Burkhard Raguse, and Lech Wieczorek

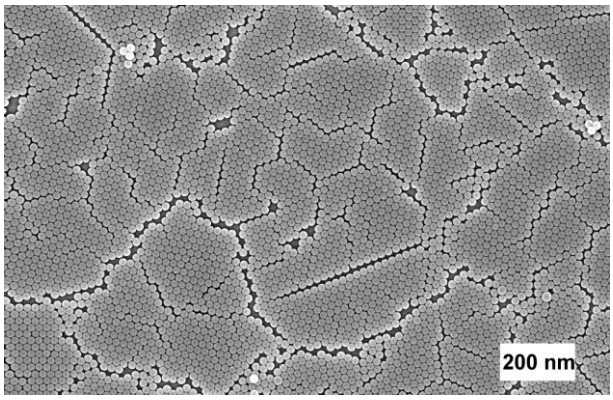

Figure S1. Low magnification scanning electron microscope image of a typical coating showing how the regular ordering of the spheres is interrupted with domain boundaries spaced some tens of micrometers apart.

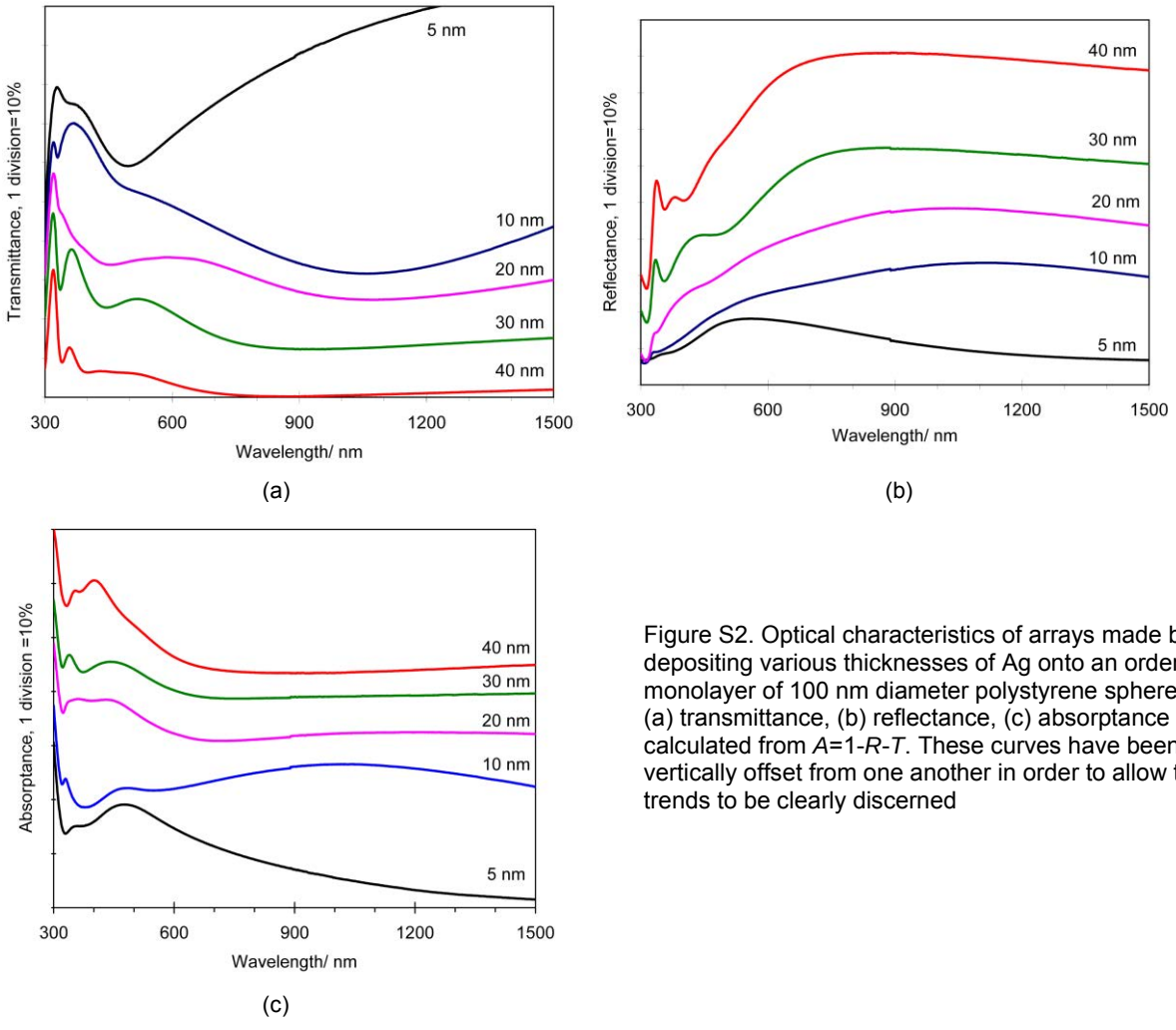

Figure S2. Optical characteristics of arrays made by depositing various thicknesses of Ag onto an ordered monolayer of 100 nm diameter polystyrene spheres, (a) transmittance, (b) reflectance, (c) absorptance calculated from A=1-R-T. These curves have been vertically offset from one another in order to allow the trends to be clearly discerned

.

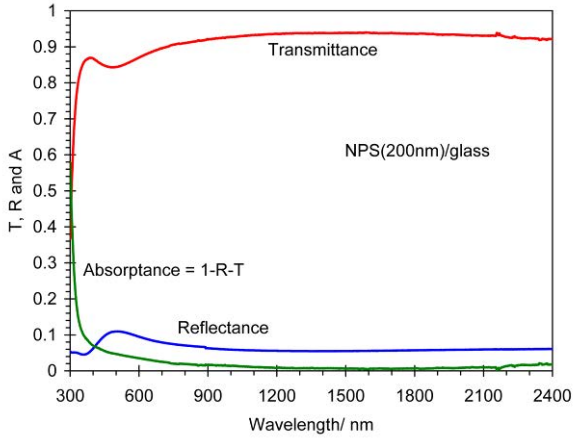

Figure S3. Optical characteristics of ordered monolayer of bare 200 nm diameter polystyrene spheres on glass

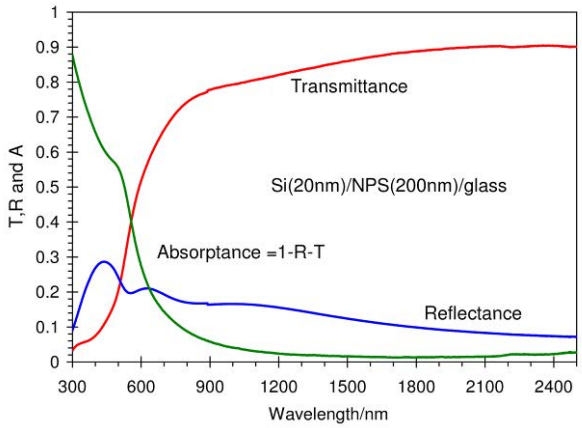

Figure S4. Optical characteristics of 20 nm Si deposited onto ordered monolayer of 200 nm polystyrene spheres.

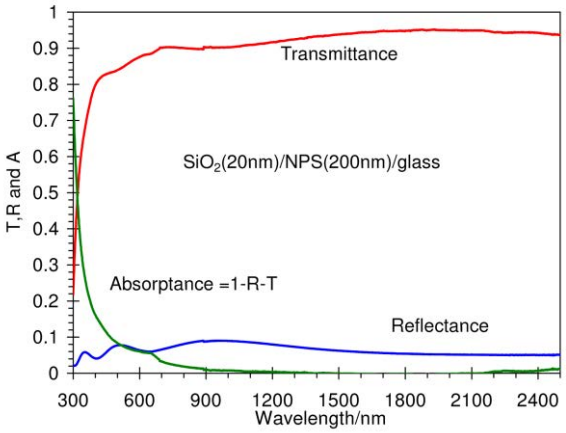

Figure S5. Optical characteristics of 20 nm SiO_2 deposited onto ordered monolayer of 200 nm polystyrene spheres.

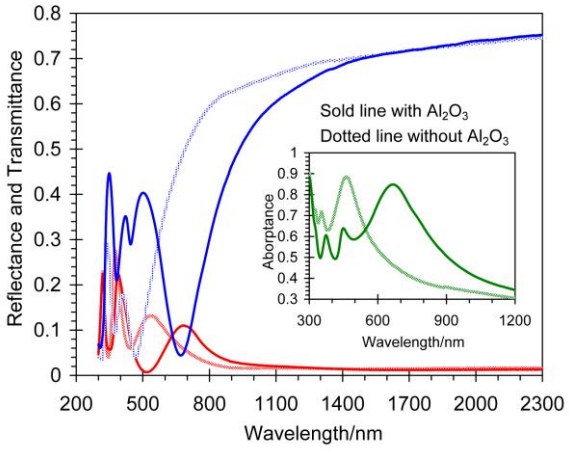

Figure S6. Red-shift in absorption peaks when a 20 nm Ag-on-200nm-PSN array is over-coated in turn with Al_2O_3.

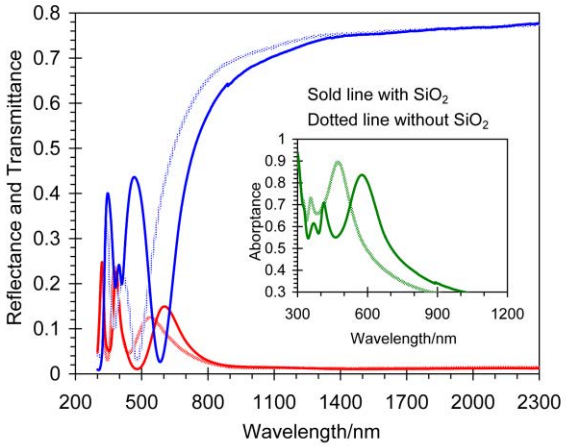

Figure S7. Red-shift in absorption peaks when a 20 nm Ag-on-200nm-PSN array is over-coated in turn with SiO_2.

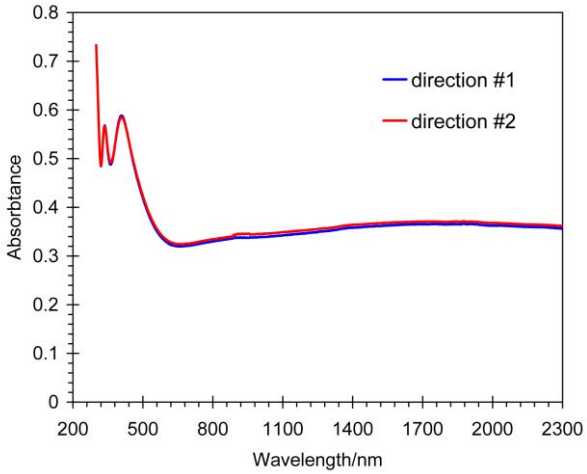

Figure S8. Effect of azimuthal rotation on the absorbtance of a coating produced by depositing 20 nm of Ag onto a layer of 100 nm diameter polystyrene nanospheres, on glass.

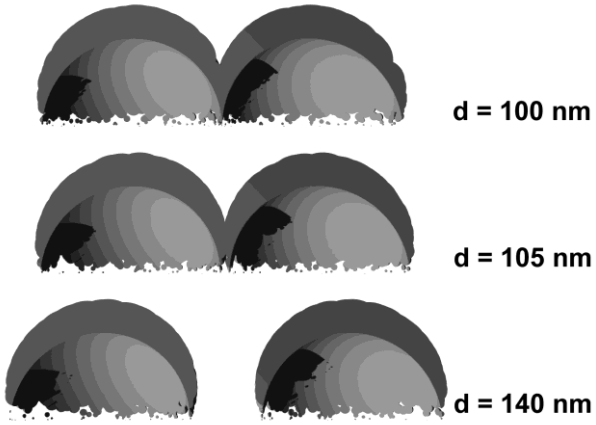

(a)

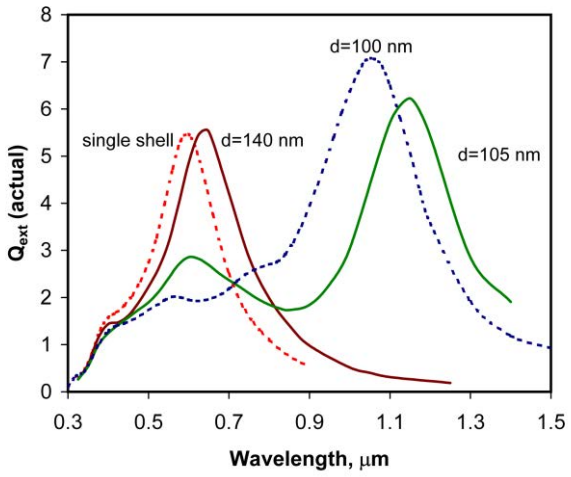

(b)

Figure S9. Effect of the nature of the ligament or 'neck' between two adjacent semishells on the propagation of the β (longitudinal) plasmon resonance. (a) Cross-sections through Ag targets used in the simulation. Each target has an internal diameter of 100 nm and is coated with a maximum of 20 nm Ag. The centre-to-centre distances of the three targets used are 100 nm, 105 nm and 140 nm. (b) Calculated optical extinction efficiencies of the three targets, with polarization of light as shown in Figure 10 of main paper.